LETTER

doi:10.1038/nature13433

Precision measurement of the Newtonian gravitational constant using cold atoms

G. Rosi[1], F. Sorrentino[1], L. Cacciapuoti[2], M. Prevedelli[3] & G. M. Tino[1]

About 300 experiments have tried to determine the value of the Newtonian gravitational constant, *G*, so far, but large discrepancies in the results have made it impossible to know its value precisely[1]. The weakness of the gravitational interaction and the impossibility of shielding the effects of gravity make it very difficult to measure *G* while keeping systematic effects under control. Most previous experiments performed were based on the torsion pendulum or torsion balance scheme as in the experiment by Cavendish[2] in 1798, and in all cases macroscopic masses were used. Here we report the precise determination of *G* using laser-cooled atoms and quantum interferometry. We obtain the value $G = 6.67191(99) \times 10^{-11}\ \mathrm{m^3\,kg^{-1}\,s^{-2}}$ with a relative uncertainty of 150 parts per million (the combined standard uncertainty is given in parentheses). Our value differs by 1.5 combined standard deviations from the current recommended value of the Committee on Data for Science and Technology[3]. A conceptually different experiment such as ours helps to identify the systematic errors that have proved elusive in previous experiments, thus improving the confidence in the value of *G*. There is no definitive relationship between *G* and the other fundamental constants, and there is no theoretical prediction for its value, against which to test experimental results. Improving the precision with which we know *G* has not only a pure metrological interest, but is also important because of the key role that *G* has in theories of gravitation, cosmology, particle physics and astrophysics and in geophysical models.

The basic idea of our experiment is to use an atom interferometer as a gravity sensor and a well-characterized mass as the source of a gravitational field. From the precise measurement of the atoms' acceleration produced by the source mass and from the knowledge of the mass distribution, it is possible to extract the value of *G* using the formula

$$F(r) = -G\frac{M_1 M_2}{r^2}\hat{r}$$

where $\hat{r}$ is the radial unit vector.

Atom interferometers[4,5] are new tools for experimental gravitation, for example in precision measurements of gravitational acceleration[6] and gravity gradients[7], as gyroscopes based on the Sagnac effect[8], for testing the $1/r^2$ law[9], in general relativity[10] and quantum gravity models[11], and in applications in geophysics[12]. Proof-of-principle experiments to measure *G* using atom interferometry have been reported[13–15]. Ongoing studies show that future experiments in space will take full advantage of the potential sensitivity of atom interferometers for fundamental physics tests[16]. The possibility of using atom interferometry for gravitational wave detection is being studied[17].

Because the problem in the determination of *G* depends on the presence of unidentified systematic errors, our experiment was designed with a double-differential configuration to be as insensitive as possible to such effects: the atomic sensor was a double interferometer in a gravity gradiometer configuration, to subtract common-mode spurious signals, and to produce the gravitational field we used two sets of well-characterized tungsten masses that were placed in two different positions to modulate the relevant gravitational signal. An additional cancellation of common-mode spurious effects was obtained by reversing the direction of the two-photon recoil used to split and recombine the wave packets in the interferometer[18]. Efforts were devoted to the control of systematics related to atomic trajectories, the positioning of the atoms and effects due to stray fields. The high density of tungsten was instrumental in maximizing the signal and in compensating for the Earth's gravitational gradient in the region containing the atom interferometers, thus reducing the sensitivity of the experiment to the vertical position and size of the atomic probes.

The atom interferometer is realized using light pulses to stimulate ^{87}Rb atoms at the two-photon Raman transition between the hyperfine levels $F = 1$ and $F = 2$ of the ground state[19]. The light field is generated by two counter-propagating laser beams with wave vectors k_1 and $k_2 \approx -k_1$ aligned along the vertical direction. The gravity gradiometer consists of two vertically separated atom interferometers operated in differential mode. Two atomic clouds launched along the vertical direction are simultaneously interrogated by the same $\pi/2$–π–$\pi/2$ pulse sequence. The difference in the phase shifts detected at the output of each interferometer provides a direct measurement of the differential acceleration induced by gravity on the two atomic samples. In this way, any spurious acceleration induced by vibrations or seismic noise in the common reference frame identified by the vertical Raman beams is efficiently rejected.

Figure 1 shows a sketch of the experiment. The atom interferometer apparatus and the source mass assembly are described in detail elsewhere[20,21]. In the vacuum chamber at the bottom of the apparatus, a magneto-optical trap (MOT) collects $\sim 10^9$ rubidium atoms. After turning the MOT magnetic field off, the atoms are launched vertically along the symmetry axis of the vacuum tube by using the 'moving-molasses' technique. During the launch sequence, atoms are laser cooled to a temperature of $\sim 4\ \mu$K. We juggle two atomic samples to have them reach the apogees of their ballistic trajectories at about 60 and, respectively, 90 cm above the MOT, with a vertical separation of 328 mm.

The atoms are velocity-selected and prepared in the magnetic-field-insensitive $|F = 1, m_F = 0\rangle$ hyperfine state with a combination of three π Raman pulses and two resonant laser pulses used to remove the atoms occupying the wrong hyperfine state. The interferometers are realized at the centre of the vertical tube shown in Fig. 1. In this region, surrounded by two cylindrical magnetic shields, a uniform magnetic field of 29 μT along the vertical direction defines the quantization axis. Here atoms are subjected to the Raman three-pulse interferometer sequence. The central π pulse occurs about 6 ms after the atoms reach the apogees of their trajectories. At the end of the atoms' ballistic flight, the population of the ground state is measured by selectively exciting the atoms in both hyperfine levels of the ground state and detecting the light-induced fluorescence emission. We typically detect 10^5 atoms on each rubidium sample at the end of the interferometer sequence. Each measurement takes 1.9 s. The information on the relative phase shift between the two atom interferometers is extracted from the Lissajous curve that is obtained when the signal of one interferometer is plotted as a function of the signal

[1]Dipartimento di Fisica e Astronomia and LENS, Università di Firenze - INFN Sezione di Firenze, Via Sansone 1, 50019 Sesto Fiorentino, Italy. [2]European Space Agency, Keplerlaan 1, PO Box 299, 2200 AG Noordwijk ZH, The Netherlands. [3]Dipartimento di Fisica, Università di Bologna, Via Irnerio 46, 40126, Bologna, Italy.

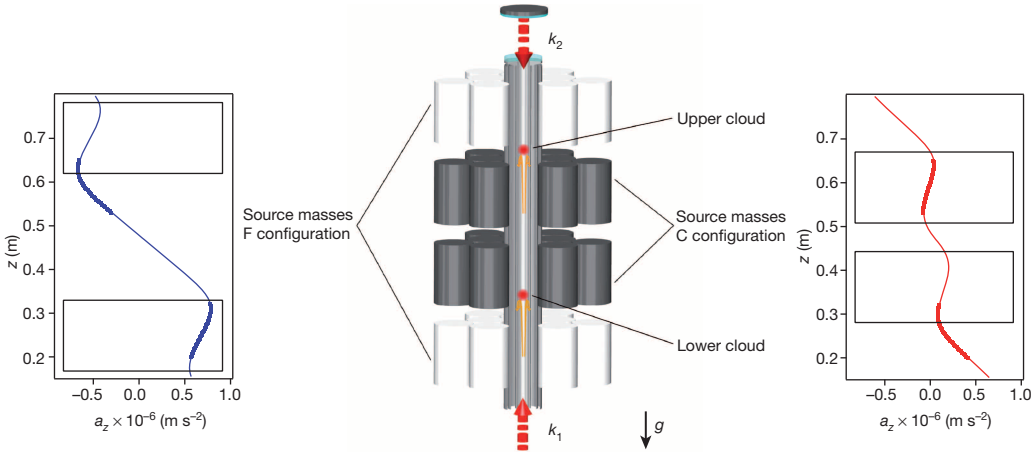

Figure 1 | Sketch of the experiment. The Rb atom interferometer operates as a gravity gradiometer and the W masses are used as the source of the gravitational field. For the measurement of G, the position of the source masses is alternated between configurations F and C. Plots of gravitational acceleration (a_z) produced along the symmetry axis by the source masses are also shown for each configuration; a constant value for Earth's gravity was subtracted. The spatial regions of the upper and lower atom interferometers are indicated by the thick lines. The vertical acceleration plots show the effect of source mass in cancelling the local gravity gradient at the positions of the atomic apogees.

of the other. Experimental points are distributed around an ellipse. The differential phase shift is extracted from the eccentricity and the rotation angle of the ellipse fitting the data[22]. The instrument sensitivity for differential acceleration is $3 \times 10^{-9} g$ for 1 s of integration (g is the acceleration due to Earth's gravity).

The source mass is composed of 24 tungsten alloy cylinders, for a total mass of about 516 kg. Each cylinder is machined to have a diameter of 99.90 mm and a height of 150.11 mm. They are positioned on two titanium platforms and distributed with hexagonal symmetry around the vertical axis of the tube (Fig. 1). The cylinders' centres lie around two circles with nominal radii $2R$ and $2R\sqrt{3}$, respectively, where R is the radius of a single cylinder. The vertical positioning of the two platforms is ensured by precision screws synchronously driven by stepper motors and by an optical readout system. The reproducibility of the positioning was verified with a laser tracker to be within 1 μm (ref. 20). With respect to the position of the apogee of the lower atomic cloud, the centres of the lower and upper sets of cylinders lie at respective vertical distances of 40 and 261 mm in one configuration (the C configuration) and at −74 and 377 mm in another (the F configuration).

The value of the Newtonian gravitational constant was obtained from a series of gravity gradient measurements performed by periodically changing the vertical position of the source masses between configurations

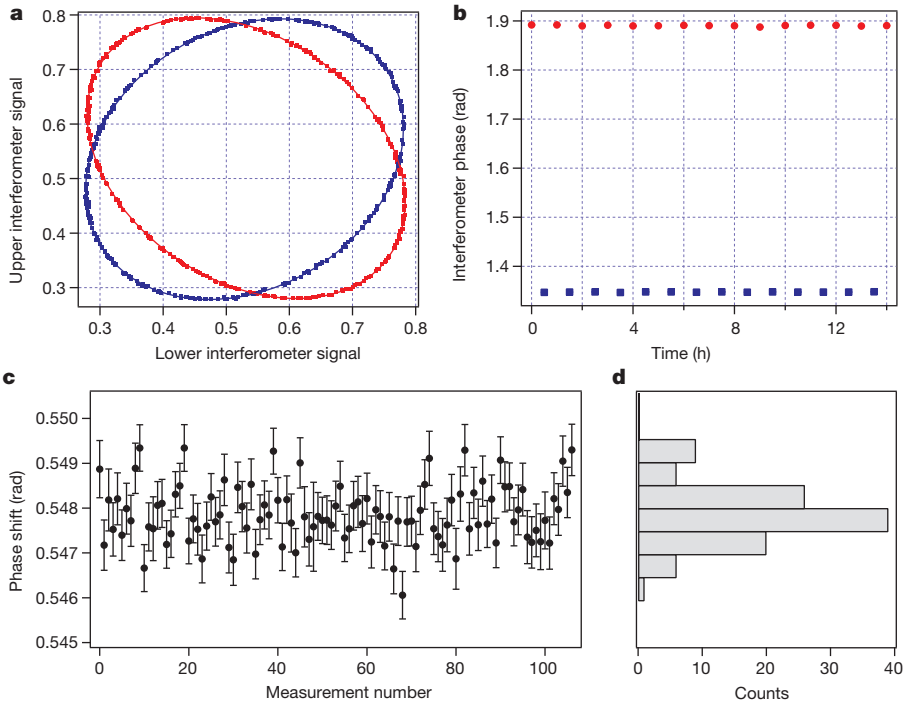

Figure 2 | Experimental data. **a**, Typical Lissajous figures obtained by plotting the output signal of the upper atom interferometer versus that of the lower one for the two configurations of the source masses. **b**, Modulation of the differential phase shift for the two configurations of source masses for a given direction of the Raman beams' k vector. Each phase measurement is obtained by fitting a 360-point scan of the atom interference fringes to an ellipse. The error bars, not visible on this scale, are given by the standard error of the least-squares fit to the ellipse. **c**, Results of the measurements to determine G. Each point is obtained by averaging the signals recorded for the two directions of the Raman k vector (Methods). Data acquisition for each point took about one hour. These data were recorded on different days during one week in July 2013. The error bars are given by the combined errors in the phase angles of four ellipses. **d**, Histogram of the data in **c**.

Table 1 | Effects, relative corrections and uncertainties considered in our determination of *G*

Parameter	Uncertainty in parameter	Relative correction to *G* (p.p.m.)	Relative uncertainty in *G* (p.p.m.)
Air density	10%	60	6
Apogee time	30 μs	—	6
Atomic cloud horizontal size	0.5 mm	—	24
Atomic cloud vertical size	0.1 mm	—	56
Atomic cloud horizontal position	1 mm	—	37
Atomic cloud vertical position	0.1 mm	—	5
Atom launch direction change C/F	8 μrad	—	36
Cylinder density homogeneity	10^{-4}	91	18
Cylinder radial position	10 μm	—	38
Ellipse fit	—	−13	4
Size of detection region	1 mm	—	13
Support platform mass	10 g	—	5
Translation stage position	0.5 mm	—	6
Other effects	—	<2	1
Total systematic uncertainty	—	—	92
Statistical uncertainty	—	—	116
Total	—	137	148

Uncertainties are quoted as one standard deviation. The third column contains the corrections we applied to account for effects not included in the Monte Carlo simulation. The bias and systematic error from ellipse fitting are evaluated by a numerical simulation on synthetic data. Other effects include cylinder mass, cylinder vertical position, gravity gradient, gravity acceleration, Raman mirror tilt, Raman *k* vector and timing.

C and F. Figure 2 shows the data used for the determination of *G*. Data were collected in 100 h during one week in July 2013. Each phase measurement was obtained by fitting a 360-point scan of the atom interference fringes to an ellipse. The modulation of the differential phase shift produced by the source mass is easily visible and could be resolved with a signal-to-noise ratio of 1,000 after about one hour. The resulting value of the differential phase shift is 0.547870(63) rad, and it was from this that we obtained *G*. The cylinders produce 97.0% of the measured differential phase shift, the cylinder supports produce 2.8% (ref. 20) and the additional moving masses (translation stages, optical rulers, screws) produce the remaining 0.2%.

The sources of uncertainty affecting the value of *G* are presented in Table 1. Positioning errors account for uncertainties in the positions of the 24 tungsten cylinders along the radial and vertical direction, both in configuration C and configuration F. Density inhomogeneities in the source masses were measured by cutting and weighing a spare cylinder[20], and were modelled in the data analysis. Precise knowledge of the atomic trajectories is of key importance in analysing the experimental results and deriving the value of *G*. The velocities of the atomic clouds, and their positions at the time of the first interferometer pulse, were calibrated by time-of-flight measurements and by detecting the atoms when they crossed a horizontal light sheet while moving upwards and downwards. The Earth's rotation affects the atom interferometers' signals because of the transverse velocity distribution of the atoms. Following the method demonstrated for a single interferometer[23,24], we implemented a tip–tilt scheme for the mirror retroreflecting the Raman beams in our double interferometer.

Extracting the value of *G* from the data involved the following steps: calculation of the gravitational potential produced by the source masses; calculation of the phase shift for single-atom trajectories; Monte Carlo simulation of the atomic cloud; and calculation of the corrections for the effects not included in the Monte Carlo simulation (Table 1).

After an analysis of the error sources affecting our measurement, we obtain the value $G = 6.67191(77)(62) \times 10^{-11}\ \mathrm{m^3\,kg^{-1}\,s^{-2}}$. The statistical and systematic errors, reported in parenthesis as one standard deviation, lead to a combined relative uncertainty of 150 p.p.m. In Fig. 3, this result is compared with the values of recent experiments and Committee on Data for Science and Technology (CODATA) adjustments. Our value,

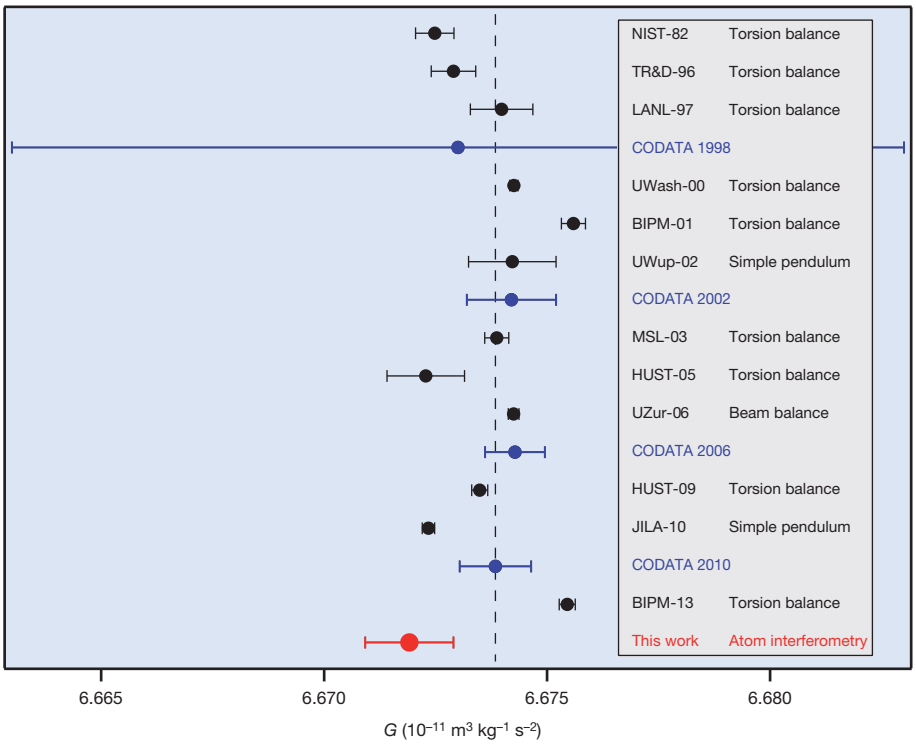

Figure 3 | Comparison with previous results. Result of this experiment for *G* compared with the values obtained in previous experiments and with the recent CODATA adjustments. Only the experiments considered for the current CODATA 2010 value, and the subsequent BIPM-13 result, are included. For details on the experiments and their identification with the abbreviations used in the figure, see ref. 3 and the additional references in Methods.

obtained with a method completely different from the ones used before, differs by 1.5 combined standard deviations from the present CODATA value, $G = 6.67384(80) \times 10^{-11}\ \mathrm{m^3\,kg^{-1}\,s^{-2}}$.

Conceptually different experiments such as ours will help to identify the errors that produced the remaining discrepancies among previous measurements. Given the relevance of the gravitational constant in several fields ranging from cosmology to particle physics, and in the absence of a complete theory linking gravity to other forces, high-precision measurements based on different methods are crucial to increase our confidence in the value of G. It is possible to imagine a new generation of experiments to measure G using ultracold atoms confined in optical traps to allow their precise positioning. The remaining major contribution to the systematic uncertainty in our experiment in fact derives from the positioning of the atoms with respect to the source mass. The choice of a different atom might reduce this source of uncertainty as well as others. For example, Sr atoms can be rapidly cooled to form Bose–Einstein condensates[25], they are virtually unaffected by magnetic fields and collisional effects in their ground state, and the possibility of their precise positioning and use in gravity measurements using optical lattices has been demonstrated[26,27]. Higher-sensitivity atom interferometers with larger splitting of the atomic wave packet would enable the use of a smaller, highly homogeneous source mass such as gold or, eventually, silicon crystals. We foresee prospects for increasing the measurement accuracy in the determination of G to better than 10 p.p.m. using atoms.

METHODS SUMMARY

The Raman lasers frequencies ν_1 and ν_2 satisfy the resonance condition $\nu_2 - \nu_1 \approx 6.8$ GHz, corresponding to the separation between the $F = 1$ and $F = 2$ levels of ^{87}Rb ground state. During absorption and stimulated emission processes, the resonant light field exchanges with atoms a total momentum of $\hbar k = \hbar k_1 - \hbar k_2$ ($\hbar$ is Planck's constant divided by 2π), coupling the two states $|F = 1, p\rangle$ and $|F = 2, p + \hbar k\rangle$, where p is the initial atomic momentum. The interferometer is composed of a $\pi/2$–π–$\pi/2$ sequence of Raman pulses separated by a time $T = 160$ ms. The pulses split, redirect and recombine the wave packets, producing atom interference. At the end of the sequence, the probability of detecting atoms in $|F = 2, p + \hbar k\rangle$ is $P_2 = [1 - \cos\phi]/2$, where ϕ is the phase difference accumulated along the interferometer arms. In a uniform gravitational field, atoms experience a phase shift $\phi = k \bullet gT^2$ that can be measured and thus provides direct information on the local acceleration due to gravity. Accurate control of noise sources and systematic phase shifts is crucial to optimize the sensitivity and the long-term stability of gravity gradient measurements[28]. Active loops have been implemented to stabilize the optical intensities of the cooling, Raman and probe laser beams and the Raman mirror tilt. In this way, we reach a quantum-projection-noise-limited sensitivity to differential accelerations of $3 \times 10^{-9} g$ after 1 s of integration time and an accuracy in the measurement of G at the level of 100 p.p.m. The measured phase shift is compared with the theoretical value obtained by evaluating the action integral along the trajectories given by the solution of the Lagrange equation:

$$\phi = \frac{1}{\hbar}\oint L\,\mathrm{d}t \qquad (1)$$

Taking a perturbative approach[29], we separate the Lagrangian L into $L_0 = p^2/2m - mgz$ (m is the atomic mass) and L_1, which accounts for the contributions of both the Earth's gravity gradient and the source mass. A Monte Carlo simulation is used to evaluate the measurement results and to determine the sensitivity of the final phase angle to the relevant parameters. To this end, the key parameters entering the simulation are varied and their derivatives calculated to estimate the uncertainty in the measurement of G.

Online Content Methods, along with any additional Extended Data display items and Source Data, are available in the online version of the paper; references unique to these sections appear only in the online paper.

Received 10 January; accepted 22 April 2014.
Published online 18 June 2014.

1. Quinn, T. Measuring big *G*. *Nature* **408,** 919–921 (2000).
2. Cavendish, H. Experiments to determine the density of the Earth. *Phil. Trans. R. Soc. Lond.* **88,** 469–526 (1798).
3. Mohr, P. J., Taylor, B. N. & Newell, D. B. CODATA recommended values of the fundamental physical constants: 2010. *Rev. Mod. Phys.* **84,** 1527–1605 (2012).
4. Cronin, A. D., Schmiedmayer, J. & Pritchard, D. E. Optics and interferometry with atoms and molecules. *Rev. Mod. Phys.* **81,** 1051–1129 (2009).
5. Tino, G. M. & Kasevich, M. A. (eds) *Atom Interferometry, Proc. Int. School Phys. "Enrico Fermi", Course CLXXXVIII, Varenna 2013* (Società Italiana di Fisica and IOS Press, 2014).
6. Peters, A., Chung, K. Y. & Chu, S. Measurement of gravitational acceleration by dropping atoms. *Nature* **400,** 849–852 (1999).
7. McGuirk, J. M., Foster, G. T., Fixler, J. B., Snadden, M. J. & Kasevich, M. A. Sensitive absolute-gravity gradiometry using atom interferometry. *Phys. Rev. A* **65,** 033608 (2002).
8. Gustavson, T. L., Landragin, A. & Kasevich, M. A. Rotation sensing with a dual atom interferometer Sagnac gyroscope. *Class. Quantum Gravity* **17,** 2385–2398 (2000).
9. Ferrari, G., Poli, N., Sorrentino, F. & Tino, G. M. Long-lived Bloch oscillations with bosonic Sr atoms and application to gravity measurement at the micrometer scale. *Phys. Rev. Lett.* **97,** 060402 (2006).
10. Dimopoulos, S., Graham, P., Hogan, J. & Kasevich, M. Testing general relativity with atom interferometry. *Phys. Rev. Lett.* **98,** 111102 (2007).
11. Amelino-Camelia, G., Lämmerzahl, C., Mercati, F. & Tino, G. M. Constraining the energy-momentum dispersion relation with Planck-scale sensitivity using cold atoms. *Phys. Rev. Lett.* **103,** 171302 (2009).
12. de Angelis, M. *et al.* Precision gravimetry with atomic sensors. *Meas. Sci. Technol.* **20,** 022001 (2009).
13. Bertoldi, A. *et al.* Atom interferometry gravity-gradiometer for the determination of the Newtonian gravitational constant *G*. *Eur. Phys. J. D* **40,** 271–279 (2006).
14. Fixler, J. B., Foster, G. T., McGuirk, J. M. & Kasevich, M. Atom interferometer measurement of the Newtonian constant of gravity. *Science* **315,** 74–77 (2007).
15. Lamporesi, G., Bertoldi, A., Cacciapuoti, L., Prevedelli, M. & Tino, G. M. Determination of the Newtonian gravitational constant using atom interferometry. *Phys. Rev. Lett.* **100,** 050801 (2008).
16. Tino, G. M. *et al.* Precision gravity tests with atom interferometry in space. *Nucl. Phys. B Proc.* Suppl. **243–244,** 203–217 (2013).
17. Tino, G. M., Vetrano, F. & Lämmerzahl, C. Editorial on the special issue on "gravitational waves detection with atom interferometry". *Gen. Relativ. Gravit.* **43,** 1901–1903 (2011).
18. Louchet-Chauvet, A. *et al.* The influence of transverse motion within an atomic gravimeter. *New J. Phys.* **13,** 065025 (2011).
19. Kasevich, M. & Chu, S. Atomic interferometry using stimulated Raman transitions. *Phys. Rev. Lett.* **67,** 181–184 (1991).
20. Lamporesi, G. *et al.* Source masses and positioning system for an accurate measurement of *G*. *Rev. Sci. Instrum.* **78,** 075109 (2007).
21. Sorrentino, F. *et al.* Sensitive gravity-gradiometry with atom interferometry: progress towards an improved determination of the gravitational constant. *New J. Phys.* **12,** 095009 (2010).
22. Foster, G. T., Fixler, J. B., McGuirk, J. M. & Kasevich, M. A. novel method of phase extraction between coupled atom interferometers using ellipse-specific fitting. *Opt. Lett.* **27,** 951–953 (2002).
23. Hogan, J., Johnson, D. & Kasevich, M. in *Proc. Int. School Phys. "Enrico Fermi", Course CLXVIII* (eds Arimondo, E., Ertmer, W., Schleich, W. & Rasel, E.) 411–447 (SIF, Bologna and IOS Press, 2009).
24. Lan, S.-Y., Kuan, P.-C., Estey, B., Haslinger, P. & Müller, H. Influence of the Coriolis force in atom interferometry. *Phys. Rev. Lett.* **108,** 090402 (2012).
25. Stellmer, S., Pasquiou, B., Grimm, R. & Schreck, F. Laser cooling to quantum degeneracy. *Phys. Rev. Lett.* **110,** 263003 (2013).
26. Sorrentino, F. *et al.* Quantum sensor for atom-surface interactions below 10 μm. *Phys. Rev. A* **79,** 013409 (2009).
27. Poli, N. *et al.* Precision measurement of gravity with cold atoms in an optical lattice and comparison with a classical gravimeter. *Phys. Rev. Lett.* **106,** 038501 (2011).
28. Sorrentino, F. *et al.* Sensitivity limits of a Raman atom interferometer as a gravity gradiometer. *Phys. Rev. A* **89,** 023607 (2014).
29. Storey, P. & Cohen-Tannoudji, C. The Feynman path integral approach to atomic interferometry. A tutorial. *J. Phys. II France* **4,** 1999–2027 (1994).

Acknowledgements G.M.T. acknowledges discussions with M. A. Kasevich and J. Faller and useful suggestions by A. Peters in the initial phase of the experiment. We are grateful to A. Cecchetti and B. Dulach for the design of the source mass support and to A. Peuto, A. Malengo, and S. Pettorruso for density tests on the tungsten masses. We thank D. Wiersma for a critical reading of the manuscript. This work was supported by INFN (MAGIA experiment).

Author Contributions G.M.T. had the idea for the experiment, supervised it and wrote the manuscript. G.R., F.S. and L.C. performed the experiment. M.P. contributed to the experiment and analysed the data.

Author Information Reprints and permissions information is available at www.nature.com/reprints. The authors declare no competing financial interests. Readers are welcome to comment on the online version of the paper. Correspondence and requests for materials should be addressed to G.M.T. (guglielmo.tino@fi.infn.it).

METHODS

Experimental set-up. Our interferometer uses Raman pulses to drive ^{87}Rb atoms on the two-photon transition between the hyperfine levels $|1\rangle \equiv |F=1, m_F=0\rangle$ and $|2\rangle \equiv |F=2, m_F=0\rangle$ of the ground state[19]. The light field is generated by two counter-propagating laser beams with wave vectors k_1 and $k_2 \approx -k_1$ aligned along the vertical direction. This configuration is obtained by retroreflecting the Raman lasers using a mirror placed on top of the vertical tube (Fig. 1). The laser frequencies ν_1 and ν_2 satisfy the resonance condition $\nu_2 - \nu_1 = \nu_0 + \nu_{AC} + \nu_{rec}$, where $h\nu_0$ is the energy corresponding to the $|1\rangle \rightarrow |2\rangle$ transition, $h\nu_{AC}$ accounts for the a.c. Stark effect and $h\nu_{rec}$ is the energy shift due to the two-photon recoil. As a consequence, the transition modifies both the internal energy and the total momentum of the atom, coupling the two atomic states $|1, p\rangle$ and $|2, p + \hbar k\rangle$, where $k = k_1 - k_2$ is the effective wavevector of the Raman transition. The $\hbar k$ momentum transfer is responsible for the spatial separation of the atomic wave packet along the two physical arms of the interferometer. During interferometry, a sequence of three Raman pulses provides the atom-optical elements of a typical Mach–Zehnder configuration: at $t = 0$ a $\pi/2$ beam-splitter pulse prepares the atoms, initially in $|1, p\rangle$, in an equal and coherent superposition of $|1, p\rangle$ and $|2, p + \hbar k\rangle$; after a time $T = 160$ ms a π pulse plays the part of a mirror, swapping state $|1, p\rangle$ with $|2, p + \hbar k\rangle$ and redirecting the atoms towards the output ports of the interferometer; at $t = 2T$ a final $\pi/2$ pulse recombines the atomic wave packets in the two output ports, where they interfere. When interacting with the light field, the phase of the Raman lasers is imprinted on the atomic wavefunction, sampling the atomic motion at the three interaction events of the $\pi/2$–π–$\pi/2$ sequence. This information can be read through the effect of matter-wave interference by detecting the atomic population in the $F = 1$ and $F = 2$ hyperfine states. If ϕ is the phase difference accumulated by the atoms along the two interferometer arms, the probability of detecting atoms in $|2\rangle$ can be expressed as $P_2 = [1 - \cos\phi]/2$. In the presence of a gravity field, atoms experience a phase shift $\phi = k \bullet gT^2$. Measuring ϕ is therefore equivalent to a measurement of the local acceleration due to the gravitational field along the direction of the effective wavevector, k.

Our instrument is a gravity gradiometer consisting of two Raman-pulse interferometers simultaneously probing two clouds of laser-cooled ^{87}Rb atoms aligned along the vertical axis and separated by a distance of 328 mm (refs 21, 28). The two atomic clouds are interrogated by the same Raman lasers with the same interferometric pulse sequence. The difference in the phase shifts at each interferometer provides a direct measurement of the differential acceleration induced by gravity on the two atomic samples. This configuration allows a very efficient rejection of common-mode noise sources, including spurious accelerations at the instrument platform induced by mechanical vibrations or seismic noise, g variations due to tidal effects and phase noise introduced by the Raman lasers. In addition, the difference in the measurements performed in configurations C and F (Fig. 1) efficiently rejects long-term systematic drifts which do not depend on the distribution of the source masses. They include wavefront distortions, magnetic field perturbations, Coriolis acceleration and light shift.

Controlling sources of statistical noise and systematic phase shifts in the gravity gradient measurement is crucial for the experiment[28]. Inertial effects induced by the Earth's rotation are an important source of both noise and systematic errors. Gravity gradient measurements are indeed sensitive to the Coriolis acceleration when differential velocities along the east–west direction are present between the two atomic samples and when the launch direction itself is not stable. Precise control of the effects of the Coriolis acceleration is achieved by applying a uniform rotation rate to the retroreflecting Raman mirror by means of PZT actuators during the atom interferometry sequence[23,24]. The optimal rotation rate, counteracting the local projection of the Earth's rotation rate on the horizontal plane, is determined to better than 2 μrad s^{-1} after maximizing the interferometers' contrast and minimizing the noise in the differential phase measurements. Under such conditions, the residual shift amounts to $1.5\Delta\theta$, where $\Delta\theta$ is the variation in the launch direction expressed in radians when switching from configuration C to configuration F, and vice versa. As a consequence, a G measurement down to the 100 p.p.m. level requires control of the launch direction to better than 37 μrad. We can control $\Delta\theta$ to better than 8 μrad. The velocity distribution of the atoms due to the finite temperature of the sample (~4 μK) also contributes a systematic shift in the G measurement. In our experiment, the Raman mirror tilt is controlled to better than 100 nrad, bringing the corresponding error in the G measurement to negligible levels. Magnetic fields can perturb atom interferometry measurements both through their mechanical action on the atomic trajectories and via the second-order Zeeman effect. A 10^3 shielding factor to external magnetic fields is achieved in the interferometer volume by passively isolating the vertical tube through a system of two cylindrical μ-metal layers. In addition, systematic shifts that slowly change over a typical timescale of a few seconds and that do not depend on the direction of the effective wavevector, k, are efficiently cancelled by reversing k with a frequency shift of the Raman lasers at each measurement cycle and taking the average phase shift[18]. They include the second-order Zeeman effect as well as the first-order light shift. Finally, the main parameters of the experiment have been actively stabilized to optimize the sensitivity and the long-term stability of gravity gradient measurements: the optical intensities of the cooling, Raman and probe laser beams are regulated by acting on the radio-frequency power driving the acousto-optical modulators, and the Raman mirror tilt is controlled by a piezo tip–tilt system. In this way, we obtain a sensitivity to differential accelerations of $3 \times 10^{-9} g$ for an integration time of 1 s, in agreement with the calculated quantum projection noise limit for 2×10^5 atoms[28].

Monte Carlo simulation and measurement systematics. Gravity gradient measurements are compared with a numerical simulation that evaluates the gravitational potential produced by a given configuration of the source masses, implements the calculation of the phase shift experienced by single atoms at the two interferometers, and finally runs a Monte Carlo simulation on the atomic trajectories by varying the initial position and velocity out of the density and velocity distribution of the atomic cloud that best fits the experimental density profiles. The gravitational potential generated by the source masses is computed analytically using a multipole expansion. The formula has been verified by calculating the potential of a single cylindrical mass along the classical path of the atoms during the interferometric sequence and comparing it against the numerical evaluation of the exact solution. The multipole expansion has been found to introduce negligible error while drastically reducing the computation time. The phase shift ϕ for an atom is obtained as $1/\hbar$ times the classical action, evaluated along the integration paths given by the solution of the Lagrange equation (equation (1)). We use a perturbative method[29] separating the Lagrangian L into $L_0 = p^2/2m - mgz$ (m is the atomic mass) and L_1, which accounts for the contributions of both the Earth's gravity gradient and the source mass. The phase shift due to L_1 is then calculated by integration over the unperturbed path given by the solution of the Lagrange equation for L_0. This approximation gives a negligible error in the determination of G because the ratio $|L_1/L_0|$ computed along the unperturbed paths is less than 10^{-7} in our experiment. The validity of the perturbative approach was additionally checked by comparison with the exact solution for the case of a uniform gradient[30]. The interaction processes between the atom and the Raman laser beams during the interferometry sequence are modelled in the code to account for the finite duration of the Raman pulses. At detection, we evaluate the convolution effects due to both the finite width of the detection beams and the finite bandwidth of the photodiodes collecting the fluorescence light in the $F = 1$ and $F = 2$ channels. Crucial for the Monte Carlo simulation is the spatial and momentum distribution used to describe the atomic sample and its evolution through the velocity selection pulses and the atom interferometer pulse sequence. Different techniques have been used to characterize the density and velocity profile of the atomic clouds. In particular, time-of-flight measurements provide the required information along the vertical direction, while the profiles in the horizontal plane are measured both by performing CCD imaging and by scanning the atomic cloud using the vertical Raman laser beams with a reduced diameter of 4 mm. The experimental data show that the spatial and velocity profiles of atomic clouds at launch, right after release from the magneto-optical trap, are well described by Gaussian distributions with spatial deviation ~3 mm and velocity deviation ~16 mm s^{-1} for the lower cloud and ~22 mm s^{-1} for the upper cloud. The velocity selection during interferometry reduces the vertical velocity deviation to ~3 mm s^{-1} and the horizontal velocity deviation to ~6 mm s^{-1}. Average transverse velocities are less than 1.5 mm s^{-1}.

The Monte Carlo simulation is used not only to evaluate the results of our measurements, but also to determine the sensitivity of the final phase angle to the relevant parameters and to estimate the uncertainty in the G measurement. Derivatives are computed with respect to 28 parameters, including the positions of the source masses; the positions and velocities of the upper and lower clouds and their times of flight at detection; the Gaussian widths of the detection lasers and their positions with respect to the atomic clouds; the interferometry sequence duration, $2T$; the effective wavevector, k, of the Raman lasers; and the gravitational acceleration and its gradient. From an analysis of the results, the spread of the atomic sample along the vertical direction appears to be responsible for the dominant contribution, requiring a measurement of the Gaussian width for both the upper and lower clouds to better than 0.1 mm. The determination of the atomic trajectories requires a good knowledge of the local gravitational acceleration and of the gravity gradient. Gravitational acceleration was measured by using an absolute gravimeter to an uncertainty that contributes a negligible error to the G measurement. A recent measurement of the gravity gradient performed with our atom interferometer gave 3.11×10^{-6} s^{-2}, with an effect of less than 2 p.p.m. on the determination of the Newtonian gravitational constant. The G measurement has been corrected for the effect of the finite density of the volume of air that replaces the source masses when they are moved from configuration C to configuration F, and vice versa. The corresponding correction to the G value amounts to $+60 \pm 6$ p.p.m. Finally, a correction has been applied to account for the non-uniform density of the tungsten cylinders[20];

the axial density inhomogeneity of the cylinders gives the main contribution, corresponding to a correction to the G value of $+90 \pm 20$ p.p.m.

The uncertainty budget of our measurement of the Newtonian gravitational constant is detailed in Table 1. Our result is reported in Fig. 3 and compared with the CODATA value[3] and recent determinations for G (refs 31–43).

30. Antoine, C. & Bordé, C. Exact phase shifts for atom interferometry. *Phys. Lett. A* **306,** 277–284 (2003).
31. Luther, G. G. & Towler, W. R. Redetermination of the Newtonian gravitational constant *G*. *Phys. Rev. Lett.* **48,** 121–123 (1982).
32. Karagioz, O. & Izmailov, V. Measurement of the gravitational constant with a torsion balance. *Meas. Tech.* **39,** 979–987 (1996).
33. Bagley, C. H. & Luther, G. G. Preliminary results of a determination of the Newtonian constant of gravitation: a test of the Kuroda hypothesis. *Phys. Rev. Lett.* **78,** 3047–3050 (1997).
34. Gundlach, J. H. & Merkowitz, S. M. Measurement of Newton's constant using a torsion balance with angular acceleration feedback. *Phys. Rev. Lett.* **85,** 2869–2872 (2000).
35. Quinn, T. J., Speake, C. C., Richman, S. J., Davis, R. S. & Picard, A. A new determination of *G* using two methods. *Phys. Rev. Lett.* **87,** 111101 (2001).
36. Kleinevoss, U. *Bestimmung der Newtonschen Gravitationskonstanten G*. PhD thesis, Univ. Wuppertal (2002).
37. Armstrong, T. R. & Fitzgerald, M. P. New measurements of *G* using the measurement standards laboratory torsion balance. *Phys. Rev. Lett.* **91,** 201101 (2003).
38. Hu, Z.-K., Guo, J.-Q. & Luo, J. Correction of source mass effects in the HUST-99 measurement of *G*. *Phys. Rev. D* **71,** 127505 (2005).
39. Schlamminger, S. *et al.* Measurement of Newton's gravitational constant. *Phys. Rev. D* **74,** 082001 (2006).
40. Luo, J. *et al.* Determination of the Newtonian gravitational constant *G* with time-of-swing method. *Phys. Rev. Lett.* **102,** 240801 (2009).
41. Tu, L.-C. *et al.* New determination of the gravitational constant *G* with time-of-swing method. *Phys. Rev. D* **82,** 022001 (2010).
42. Parks, H. V. & Faller, J. E. Simple pendulum determination of the gravitational constant. *Phys. Rev. Lett.* **105,** 110801 (2010).
43. Quinn, T., Parks, H., Speake, C. & Davis, R. Improved determination of *G* using two methods. *Phys. Rev. Lett.* **111,** 101102 (2013).